

Naval Research Laboratory

Washington, DC 20375-5320



AD-A260 149



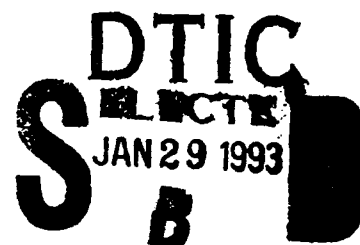
NRL/MR/7221-93-7176

**Measurement and Interpretation of the Turbulent Flow
Wall Pressure Field of a Dilute Polymer Solution Within a
Rectangular Channel Containing Smooth Walls**

MICHAEL P. HORNE

*Remote Sensing Physics Branch
Remote Sensing Division*

January 8, 1993



93-01615



25 pl

REPORT DOCUMENTATION PAGE			Form Approved OMB No. 0704-0188	
Public reporting burden for this collection of information is estimated to average 1 hour per response, including the time for reviewing instructions, searching existing data sources, gathering and maintaining the data needed, and completing and reviewing the collection of information. Send comments regarding this burden estimate or any other aspect of this collection of information, including suggestions for reducing this burden, to Washington Headquarters Services, Directorate for Information Operations and Reports, 1215 Jefferson Davis Highway, Suite 1204, Arlington, VA 22202-4302, and to the Office of Management and Budget, Paperwork Reduction Project (0704-0188), Washington, DC 20503.				
1. AGENCY USE ONLY (Leave Blank)	2. REPORT DATE January 8, 1993	3. REPORT TYPE AND DATES COVERED Final		
4. TITLE AND SUBTITLE Measurement and Interpretation of the Turbulent Flow Wall Pressure Field of a Dilute Polymer Solution Within a Rectangular Channel Containing Smooth Walls			5. FUNDING NUMBERS PE -61153N TA -RR023 01-41 WU -DN158-015	
6. AUTHOR(S) Michael P. Horned				
7. PERFORMING ORGANIZATION NAME(S) and ADDRESS(ES) Naval Research Laboratory Washington, DC 20375-5320			8. PERFORMING ORGANIZATION REPORT NUMBER NRL/MR/7221-93-7176	
9. SPONSORING/MONITORING AGENCY NAME(S) AND ADDRESS(ES) Office of Naval Research Arlington, VA 22217-5000			10. SPONSORING/MONITORING AGENCY REPORT NUMBER	
11. SUPPLEMENTARY NOTES				
12a. DISTRIBUTION/AVAILABILITY STATEMENT Approved for public release, distribution is unlimited.			12b. DISTRIBUTION CODE	
13. ABSTRACT (Maximum 200 words) Measurements of the one and two-point spectral statistics of the wall pressure field were conducted within a smooth-wall turbulent channel flow containing both Newtonian (water) and non-Newtonian liquids. The test section of the channel was located far enough downstream to insure fully developed turbulence and the high aspect ratio of the channel (18:1) provided homogeneity of the flow in the transverse direction. Single component laser Doppler velocimetry (LDV) measurements were conducted in both the Newtonian and non-Newtonian cases in order to validate the channel kinematics and aid in the interpretation of the pressure fluctuation statistics. Reynolds number effects were examined and compared to similar experimental results in the literature. Recently developed signal processing techniques were utilized to enhance the statistical quality of the wall pressure field at low frequencies and those results pertaining to the polymer flow regime are believed to be the first of such high quality. The most interesting feature indicated from the pressure statistics is the loss of information at high frequencies which contain eddies at the smallest scales. Furthermore, the pressure spectra scaled on outer variables suggest that the limits on this smallest scale can be related to the relaxation time of the polymer molecule. At the present time, it is believed that non-Newtonian fluids primarily affect the production of turbulence energy. However, results from the single point pressure statistics suggest that polymer flows enhance a fluid's ability to dampen out turbulence via dissipation. The two-point statistics show an increase in the streamwise coherence at low frequencies suggesting a higher concentration of energy is contained within the larger scale structure of the flow. These results further suggest that this energy is contained over a smaller range of scales than for its Newtonian counterpart.				
14. SUBJECT TERMS Noise Cancellation Wall Pressure Channel Flow Dilute Polymer solutions Turbulent Flow Drag Reduction			15. NUMBER OF PAGES 26	
			16. PRICE CODE	
17. SECURITY CLASSIFICATION OF REPORT UNCLASSIFIED	18. SECURITY CLASSIFICATION OF THIS PAGE UNCLASSIFIED	19. SECURITY CLASSIFICATION OF ABSTRACT UNCLASSIFIED	20. LIMITATION OF ABSTRACT UL	

CONTENTS

	Page
LIST OF FIGURES	iv
NOMENCLATURE	v
INTRODUCTION	1
DESCRIPTION OF EXPERIMENTS	1
RESULTS	4
CONCLUSIONS	7
ACKNOWLEDGEMENTS	8
REFERENCES	9

PER QUALITY INSPECTED 3

Accession For	
NTIS GRA&I	<input checked="" type="checkbox"/>
DTIC TAB	<input type="checkbox"/>
Unannounced	<input type="checkbox"/>
Justification	
By	
Distribution/	
Availability Codes	
Dist	Avail and/or Special
A-1	

LIST OF FIGURES

	Page
FIGURE 1. Rectangular Water Channel Facility.....	10
FIGURE 2. Mean Velocity Profiles For Newtonian (open symbols) and non-Newtonian (closed symbols): Law-of-the-wall-----; Log-law ———; Spalding ¹⁶; Virk ¹⁸ ———.....	11
FIGURE 3. Intensity Profiles For Newtonian (open symbols) and non-Newtonian (closed symbols): Reischman & Tiederman ¹⁵ ——— Newtonian and — . — non-Newtonian; Wilmarth <i>et al</i> ²⁰ ----- Newtonian and non-Newtonian.....	12
FIGURE 4A. Raw Spectral Output for $R_h = 15000$ With 11.8% Drag Reduction.....	13
FIGURE 4B. Raw Spectral Output for $R_h = 20000$ With 26.8% Drag Reduction.....	13
FIGURE 4C. Raw Spectral Output for $R_h = 25000$ With 32.3% Drag Reduction.....	14
FIGURE 5A. Newtonian Composite Using Outer Variables.....	15
FIGURE 5B. Polymer Composite Using Outer Variables.....	15
FIGURE 6A. Newtonian Composite Using Mixed Variables.....	16
FIGURE 6B. Polymer Composite Using Mixed Variables.....	16
FIGURE 7A. Newtonian Composite Using Inner Variables.....	17
FIGURE 7B. Polymer Composite Using Inner Variables.....	17
FIGURE 8A. Inline Correlation for $R_h = 15000$	18
FIGURE 8B. Transverse Correlation for $R_h = 15000$	19
FIGURE 9. Inline Coherence for $R_h = 15000$	20

NOMENCLATURE

A_s	channel aspect ratio, $A_s = w/2h$
B	Spalding 'log-law/law-of-the-wall' composite profile constant
d	hydraulic diameter
d_t	transducer diameter
d^+	non-dimensional transducer diameter, $d^+ = d_t u^* / \nu$
F, f	frequency (Hz)
F_{max}	maximum frequency for which turbulence information exists
h	channel half-height
k	Spalding 'log-law/law-of-the-wall' composite profile constant
LDV	laser Doppler velocimetry
p	fluctuation component of pressure
Q	average dynamic head, $Q = 1/2 \rho \bar{U}^2$
Q_o	dynamic head, $Q_o = 1/2 \rho U_o^2$
R_h	channel Reynolds number, $R_h = \bar{U} h / \nu$
S_t	Strouhal frequency, $S_t = f d / U_o$
t	time variable
t^*	viscous time unit, $t^* = \nu / u^{*2}$
\bar{U}	channel average or bulk velocity
$\bar{U}(y)$	streamwise mean velocity as a function of wall-normal distance
U_o	channel centerline velocity, (maximum velocity)
u^+	$\bar{U}(y) / u^*$
u^*	shear velocity, $u^* = \sqrt{\tau_{wall} / \rho}$
w	channel width
x, y, z	streamwise, wall-normal and spanwise coordinate directions
y^+	$y u^* / \nu$
ν	kinematic viscosity
π	3.14159.....
ρ	fluid density
τ_{wall}	wall shear stress

MEASUREMENT AND INTERPRETATION OF THE TURBULENT FLOW WALL PRESSURE FIELD OF A DILUTE POLYMER SOLUTION WITHIN A RECTANGULAR CHANNEL CONTAINING SMOOTH WALLS

INTRODUCTION

The study of drag reducing, non-Newtonian fluid flows received its initial impetus from the work of Toms [17]. Ever since Toms's innovative investigations, the examination of the turbulent flow properties of dilute solutions of high molecular weight polymers has continued at a steady pace. The markedly different flow resulting from such non-Newtonian effects has been attributed to the long chain structure of the polymers as well as the polymers' properties which are generally believed to be rate-dependent. At certain strain rates (dependent on flow velocity), the "shape" of the polymer molecule becomes anisotropic and aligns partially with the flow forming elongated structures (Hendricks *et al*, [7]). Mean velocity profiles remain unchanged for the viscous and log-law regions. On the other hand, the "buffer" region in a polymer flow becomes broader and extends farther from the wall than the Newtonian case. Similar effects are noticed in the streamwise fluctuating component of velocity with the profile becoming broader and more intense and the location of its maximum increasing and shifting away from the wall.

One area which has been only sparsely addressed in the polymer literature is the measurement of wall pressure in these types of flows. There is a historical interest in the origin of structural vibrations induced by pressure fluctuations at the surface. These vibrations contribute to surface fatigue and lead to radiated acoustic noise. Wall pressure can be considered as a "footprint" of turbulence, relating inner wall energetic small scale processes to larger scale phenomena which occur in the outer boundary layer. Although wall pressure is the summation of dynamic contributions throughout the boundary layer, its non-intrusive measurement may provide much insight into the physics of this unique flow.

DESCRIPTION OF EXPERIMENTS

Wall pressure measurements and single-component LDV measurements of the mean and fluctuating quantities of velocity were completed in a 457 mm x 25 mm (18:1 aspect ratio) rectangular channel at the Naval Research Laboratory (see figure 1). The major features of the facility are a pressure tank, upstream liquid reservoir, turbulence management section, entrance section for the developing turbulent flow, the test section and a downstream reservoir. Other than the two large tanks, the rest of the facility is enclosed within a temperature controlled, acoustically isolated laboratory. The primary advantage of this facility is that it operates in a blow-down configuration to restrict contaminating noise due to structure vibration and/or vibrationally induced acoustic phenomena, which are typical of a recirculating system.

Manuscript approved October, 27, 1992.

The measurement location was on the centerline of the channel and 4.1 m downstream from the beginning of the developing turbulent boundary layer. The ratio of downstream distance of the measurement location to the half-height of the channel, x/h , was 320. This value of x/h is well beyond that needed for fully developed turbulent channel flow as shown by Hussain & Reynolds [10]. As previously mentioned, the flow channel is a blowdown type facility and can operate at flow speeds of up to 2 m/s (average velocity). The LDV probe volume diameter was 75 μm equivalent to about 5-10 viscous units (depending on the Reynolds number), and the system was operated in backscatter mode with a counter processor. The fluid was seeded with 1.5 μm particles of silicon carbide to provide scattering material for the LDV system. Optical access was through the side plexiglas window of the channel. The optical axis was tilted slightly from the horizontal to enhance the location of the scattering volume in relation to the upper wall. In other words, leaving the laser beams parallel to the channel walls, meant the possibility of the beams being blocked as the probe volume is traversed towards the wall. By tipping the optical axis, the probe volume intersects the wall before the individual beams become blocked.

The limiting aspects of the probe volume size together with optical scattering off the plexiglas window resulted in a noise level received by the photo-multiplier. This noise level can be interpreted as an artificial turbulence intensity and prevented accurate measurements of the streamwise fluctuating component of velocity. However, these measurements are important to substantiate non-Newtonian effects and although not quantitatively accurate, excellent qualitative comparisons made be made to similar results in the literature.

Five small pressure transducers were embedded flush at the wall within a small plate in the test section. These transducers are model 8514-10 piezo-electric sensors manufactured by ENDEVCO. Their nominal sensitivities as reported by the manufacturer, were -227dB referenced to 1.0 volt/ μpa with a flat frequency response out to 140 kHz. The active area of the transducer as reported by Galib and Zandia [4], is approximately 0.5 mm. This dimension gives a ratio of channel half height to transducer diameter (h/d_t) of approximately 25/1, and a viscous scale, $d^+ = (d_t u^*)/\nu$ in the range 20 to 40. The signals from each transducer were amplified to a suitable level, low-pass filtered to prevent aliasing, simultaneously sampled in time and then digitized and stored on magnetic tapes for post processing.

The data/acquisition was accomplished with a Quad System, Inc. (QSI) 16 channel model 721 data processor. This unit includes a 12-bit A/D converter, 16 sample holds, a variable quartz clock providing sampling frequencies from 0.5 to 500kHz resulting in an overall throughput storage capability of 47,000 bytes/sec. The storage medium was a Cipher tape drive utilizing IBM compatible phase encoded (PE) formatting and stored the data as two-byte integer words in 2's complement binary on a 10 inch reel. Although the throughput limited the storage capability to only five transducers, the versatility of the system was realized by the capability of these tapes being read by any computer tape drive that can read

variable length records on 1600-bpi 10-track 1/2-inch tape. For the Reynolds numbers investigated, a sampling frequency of 4 kHz was found sufficient to contain all relevant information.

All transducer data (digitized, filtered and recorded simultaneously in time) were transferred to a VAX 780 computer. At the Naval Research Laboratory, these computers act as front end processors to a CRAY X-MP/24 super computer. The data were transferred to the CRAY through the VAX front ends and software was written to analyze the time dependent data. For each velocity run, the data were read into appropriate arrays and the respective transducer sensitivities applied immediately. This allowed for various combinations of transform size and number of ensemble averages to be investigated to extract as much statistical information as possible. This method of analysis also provided a convenient means for applying the signal processing cancellation techniques and prohibited further errors due to unmatched sensitivities from entering into the analysis. The cancellation methods employed, enhance the statistical accuracy by using a separate transducer measurement as a noise source. The concept of a Wiener Filter (Wiener [20]) is utilized to cancel coherent noise between n -pairs of transducers and is particularly effective in canceling facility generated noise which is typical in hydrodynamic flow vessels such as pipes and channels. Both the single and two-point spectral statistics may be corrected when the transducer pair are sufficiently separated to ensure no turbulent correlation. The reader is referred to Horne & Handler [8,9] for a more detailed presentation of the methodology used.

Velocity and wall pressure measurements were made in water and in aqueous solutions (60 wppm) of polyethylene oxide (Union Carbide Polyox WSR-301) in the channel. Experiments were conducted at Reynolds numbers (R_h) from 10,000 to 25,000 for the velocity runs, and between 15,000 and 25,000 for the wall pressure. In these circumstances, R_h is based on the half-height of the channel h , and \bar{U} , the channel's bulk mean velocity. The pressure gradient in the channel was measured with a differential pressure transducer and static pressure taps located every 280 mm along the entire length of the channel. The constant pressure gradient in a fully developed turbulent channel flow provides a means of obtaining a value for the average shear stress at the wall, and these values were recorded for all experimental runs. It's important to note that the velocity runs were separate from the wall pressure experiments. Duplication of instrumentation and limited data/acquisition capability prevented simultaneous measurements. However, polymer concentrations and percent drag reduction were consistent for each respective Reynolds number investigated.

Molecular weight distributions of the polyethylene oxide in the aqueous solutions were obtained by High Pressure Liquid Chromatography (HPLC) measurements. The distributions were monitored to insure that the high molecular weight content of the solutions was consistent throughout the experiments.

RESULTS

The mean (time-averaged) streamwise velocity, plotted as u^+ as a function of y^+ , is shown in figure 2. The data were normalized using u^* calculated from the pressure gradient along the channel. Plotted for comparison is a solid line representing the composite profile of Spalding [16] utilizing the constants $k = 0.40$ and $B = 5.5$, as given by Nikuradse [13]. For the non-Newtonian data, reference is made to the ultimate drag reducing profile asymptote of Virk [18],

$$u^+ = 11.7 \ln(y^+) - 17.0, \quad (1)$$

which is represented by the dashed line.

As seen in figure 2, current work agrees well with past experiments in the fully-developed, turbulent Newtonian flow case by accurately following the composite profile of Spalding.

The drag reductions obtained for the smooth-wall channel with a 60 wppm polyethylene oxide/water solution were 11% and 32% for the two Reynolds numbers reported. The drag reduced mean velocity profiles for the dilute polymer fluid are also shown in figure 2. These data are normalized with the local values for u^* measured during each run, so the classic " ΔB " shift which is characteristic of drag reduced flows, can be noted. Far away from the wall the polymer solution profiles appear parallel to the Newtonian logarithmic law whereas nearer the wall the profiles exhibit a slope significantly greater than Newtonian approaching Virk's asymptotic profile. Also evident in figure 2 is the Reynolds number dependence of these flows in agreement with previous investigations.

The values of u'/u^* as functions of y^+ for the Newtonian and non-Newtonian smooth-wall flows are presented in figure 3. For comparison, the Newtonian and non-Newtonian data of Reischman & Tiederman [15], and Wilmarth, *et al* [21], are also given. As mentioned previously, insufficient spatial resolution of the LDV close to the wall, as well as unresolved "shot noise" to the photo multiplier, resulted in a baseline noise turbulence intensity which could not be eliminated. This resulted in slightly higher turbulence intensities being recorded for both the Newtonian and non-Newtonian results. Despite this fact, the data is of sufficient quality to allow a valid relative comparison between the two flow cases. The streamwise velocity fluctuations are increased by approximately 30% with the addition of polymers. This trend is in agreement with the data of Reischman & Tiederman and Wilmarth *et al*. A shift in location of the point of maximum intensity of u'/u^* from a value of $y^+ = 15$ to about 35 is also evident, in agreement with the results of similar investigations.

Figure 4 a,b and c show the raw output of the pressure transducers for the Reynolds numbers $R_h = 15,000, 20,000$ and $25,000$ in dB vs frequency for Newtonian (water) and non-Newtonian (60 wppm Union Carbide WSR-301, Polyethylene oxide (PEO)) fluid. The data indicates a more or less uniform reduction in wall pressure intensity throughout the frequency range, with this difference increasing with Reynolds number. Furthermore (although somewhat subtle), a slight decrease in intensity is noted in the range of frequencies present, indicative of a smaller range of turbulent scales. This decrease would suggest that for a given set of flow conditions, a polymer flow dampens the available energy, dissipating it at much larger scales (lower maximum frequency) than for Newtonian flows.

Figure 5a and 5b present composite profiles of the power spectral density (PSD) of the wall pressure fluctuations for a Newtonian and non-Newtonian fluid scaled on the outer variables, ρ , d and U_o versus the nondimensional frequency fd/U_o . In these circumstances, f is the frequency (hertz), d is the hydraulic diameter based on h , and U_o is the channel centerline velocity. The effect of outer variable scaling for Newtonian flow is typically to collapse the very low frequency information ($fd/U_o < .1$). At mid-to-high frequencies, the Newtonian data in figure 5a show a Reynolds number effect in agreement with other investigations within pipes or channels. Shown for comparison, are the pipeflow results from the past work of Bakewell *et al* [1] and Clinch [2]. The quality of the present results may be noted in figure 5a by the enhanced information obtained at higher frequencies due to the smaller transducers used in this experimental work, as well as the increased resolution at low frequencies (almost a decade) which the cancellation techniques provided.

A number of theoretical and experimental wall pressure investigations have demonstrated that pressure spectra collapses in frequency ranges (over a range of flow speeds) dependent on the location of source terms contributing to the pressure field. To first order, scaling laws can be indicative of the size of certain eddies contributing to the wall pressure and which length and time scales play a major role. As mentioned previously, outer flow variables appear to collapse very low frequency (low wavenumber) spectra and inner layer variables appear to collapse high frequency (high wavenumber) spectra. The overlap region (log-law region) of a turbulent boundary layer appears to contribute over a wider mid-range of frequencies and the collapse of wall pressure spectra depends on a mixed set of variables from both the inner and outer flow.

Figure 5b shows composite profiles for the polymer flow scaled on outer variables. Several trends can be seen in the data. The Reynolds number effect is more pronounced over the mid-frequency range than for Newtonian flow. At $fd/U_o > 10$, the Reynolds number dependence disappears and all the profiles appear to collapse to a single curve. This collapse is in stark contrast to the Newtonian data. The polymers appear to lock in the available energy to larger scale structure, thus preventing a transfer of energy to the smaller scales. In Newtonian flow, it is viscosity and inner layer time/length scales which govern the scales (hence frequency) at which dissipation takes place. The addition of polymers to the flow suggests that this phenomena appears to be governed by the outer flow. It is not suggested that the transfer of

energy from big scales to small scales (cascade theory of turbulence) is not taking place. What the data of figure 5b explicitly shows is that this transfer of energy to smaller scale is "forced" to take place at a "time" scale governed by outer flow variables. This result is unique and to our knowledge, not been shown before.

Composite profiles of both the Newtonian and non-Newtonian flow results are presented in figures 6a,b and 7a,b for mixed and inner variable scaling respectively. The data of Corcos *et al* [3] and Greshilov *et al* [5] scaled with mixed variables are shown in figures 6a and 6b for comparison purposes. However, no similar data was found in the literature for internal flow configurations to compare to the results presented in figures 7a and 7b.

If one assumes that wall pressure in a non-Newtonian flow is governed by outer flow variables only, then the expected effect of introducing mixed and/or inner variable scaling is to multiply the data by a constant. Since this constant depends on flow speed, a Reynolds number dependence would be expected and is indicated in these results for the higher frequencies. It may be noted that figure 7b shows a Reynolds number dependence throughout all frequencies. This suggests that polymer effects in the fluid have shifted all turbulent transport and destruction processes to larger scale structure in the flow and that wall layer dynamics play only minor roles at defining these limits. This redistribution appears to occur at a larger scale in the polymer flow in such a way as to restrict to lower frequencies, the scale at which dissipation occurs.

In figure 6b, it can be seen that below $fd/U_o < 10$ the data collapse, with a slight Reynolds number dependence indicated at larger frequencies. In figure 5b the pressure spectra completely collapses for $fd/U_o > 10$. These data suggest that the Strouhal frequency $fd/U_o = 10$ is unique for polymer flows. It has been suggested that the time scale which depicts drag reduction is of the order of the polymer relaxation time and in fact, Lumley [12] has suggested that this value might approximately equal ten viscous time units ($t^* = \nu/u^{*2} = 10$). If one examines figure 7b and letting $f = 1/t$, we see that ten viscous time units corresponds to $f\nu/u^{*2} = 0.1$. This remarkable insight appears to be supported by observing the Reynolds number deviation at this value. Furthermore, it can be shown that for the present set of experimental data, this also corresponds to a Strouhal frequency $S_t = 10$ as previously depicted in figure 5b.

Dissipation at smaller scales for Newtonian flows is driven by inner layer length and time scales as shown by all experimental evidence to date and as depicted in figure 7a. On the other hand, the polymer results suggest that dissipation is occurring at larger scales (lower frequencies), hence it's the outer flow that forces or drives the scales at which this transfer of energy takes place and it's governed by an outer flow time scale. An explanation might be that the alignment of the polymer molecule in the flow direction together with the wider spacing of low speed streaks has resulted in larger scale structure containing most

of the energy. It is thought that pressure acts as the medium through which this energy is distributed amongst the various scales in the flow. This is supported by the work of Walker [19] and Harder & Tiederman [6] who found that the pressure-strain terms in the equation of balance of turbulent kinetic energy dominated the redistribution and/or transport processes of turbulent energy.

Figures 8a and 8b are representative plots of the two-point inline and transverse correlations at several separations for the polymer and corresponding Newtonian flows at the Reynolds number $R_h = 15,000$. The source transducer utilized for noise cancellation, ceased operating during the two-point spectral runs and resulted in the high correlations (at low time delay) indicated in these figures. However, a good qualified comparison can be made between the Newtonian and non-Newtonian flow cases. The data from both figures indicate a broader extent of correlation exists for the polymer flow. The streamwise correlation presented in figure 8a shows that the broadband convection velocity appears unchanged for the polymer flow but the decay rate for all eddies is much slower than for the Newtonian case. Figure 8b shows the correlation is also higher in the transverse direction. These results are qualitatively in agreement with the observed increase in the spacing of the low speed streaks as shown by Oldaker & Tiederman [14].

In figure 9, we present a representative plot of the streamwise coherence for three separations at the Reynolds number, $R_h = 15,000$. The coherence at all frequencies is higher with polymers, particularly for the two larger spatial separations. Since the coherence is higher throughout the frequency range, "all" structures seem to have a longer "lifetime". The effect of the polymer solution is to increase the streamwise coherence over a broad range of frequencies. This result, together with the correlation data from figures 8a and 8b, again support the thesis that there is a tendency towards larger structures existing in both streamwise and transverse orientations.

CONCLUSIONS

The increase in coherence and correlation coefficients are qualitatively consistent with the flow visualization studies of Oldaker & Tiederman [14] in which a streamwise elongation of the low-speed streaks in the wall region was noted. However, the results of Greshilov *et al.* [5] appear to contradict the results presented here. They observed a slight decrease in streamwise coherence. We suggest that the lack of proper development of coherent structures in the near wall region of their low aspect ratio (3.5:1) channel might be significant.

The reduction in the intensity of the wall pressure fluctuations throughout the frequency range investigated (particularly at low frequencies) as well as the collapse of polymer pressure spectra on outer flow time scales is new information. The measurements of the wall pressure spectral field presented here suggests a different picture of how polymers affect the turbulence. The idea of larger longer lasting structures

emerges, wherein the production, transport and dissipation of turbulence in this structurally altered flow is changed, with the wall pressure field playing a major role.

ACKNOWLEDGEMENTS

This work was supported by the Office of Naval Research (Code 11) and the Naval Research Laboratory under the Fluid Dynamics Task Area.

REFERENCES

1. Bakewell, Henry P., *et al*, "Wall Pressure Correlations in Turbulent Pipe Flow", Naval Underwater Sound Laboratory, USL Report No. 559, 1962.
2. Clinch, J.M., "Measurements of the Wall Pressure Field at the Surface of a Smooth-Walled Pipe Containing Turbulent Water Flow", *J. Sound Vibrations*, Vol 9(3), 1969.
3. Corcos, G.M., Cuthbert, J.W. and vonWinkle, W.A., "On the Measurement of Turbulent Pressure fluctuations With A Transducer of Finite Size," Univ. of California Inst. Eng. Research Report, Series 82, No. 12, Nov 1959
4. Galib, T.A. and Zandina, A., *JASA Suppl.* 1(76), 1984.
5. Greshilov, E.M., Evtushenko, A.V. & Lyamshev, L.M., "Hydrodynamic Noise and the Toms Effect", *Sov. Phys. Acoust.*, (21), pp 247-251, 1975.
6. Harder, K.J. and Tiederman, W.G., "Influence of Wall Strain Rate, Polymer Concentration and Channel Height Upon Drag Reduction and Turbulent Structure", ONR Report PME-FM-89-1, 1989.
7. Hendricks, E.W., Handler, R.A., Lawler, J.V., Horne, M.P. and Swearingen, J.D, "Experiments in Drag Reducing Polymer Flows", *Advances In Fluid Mechanics Measurements*, Ed. Mohamed Gad-El-hak, Springer-Verlag; *Lecture Notes In Engineering*, Vol. 45, pp. 535-568, 1988.
8. Horne, M.P. and Handler, R.A., "Innovative Methodology for Cancelling Contaminating Noise in Turbulent Fluid Flow Environments", NRL report. (6683), July, 1990.
9. Horne, M.P. and Handler, R.A., "Note On The Cancellation of Contaminating Noise in the Measurement of Turbulent Wall Pressure Fluctuations", *Experiments in Fluids*, 18, p200, 1991.
10. Hussain, A.K.M.F. and Reynolds, W.C., *ASME J. Fluid Engr.*, 97, p.568, 1975.
11. Luchik, T.S., Ph.D. Thesis, Purdue University, 1985.
12. Lumley, J.L., *J. Polymer Sci.: Macromolecular Reviews*, Vol. 7, 263-290, J. Wiley and Sons, Inc., 1973.
13. Nikuradse, j. *Ing.-Arch.*, (1), p. 306, 1930.
14. Oldaker, D.K. and Tiederman, W.G., *Physics of Fluids* (20), S133, 1977.
15. Reischman, M.M. and Tiederman, W.G., *J. Fluid Mech.*, (70), p. 369, 1975.
16. Spalding, D.B., *J. Appl. Mech.*, vol.28, p. 455, 1961.
17. Toms, B.A., *Proc. First International Congress on Rheology* (Amsterdam), Sec. II, p135, 1949.
18. Virk, P.S., *AIChE J.*, (21), P. 625, 1975.
19. Walker, D.T., "Turbulent Structure and Mass Transport in a Channel Flow With Polymer Injection", Ph.D. Thesis, Purdue University, 1988.
20. Wiener, N., *Extrapolation, Interpolation and Smoothing of Stationary Time Series, With Engineering Applications*, Wiley, New York, 1949.
21. Wilmarth, W.W., Wei, T. and Lee, C.O., *Phys. Fluids*, (30), p. 933, 1987.

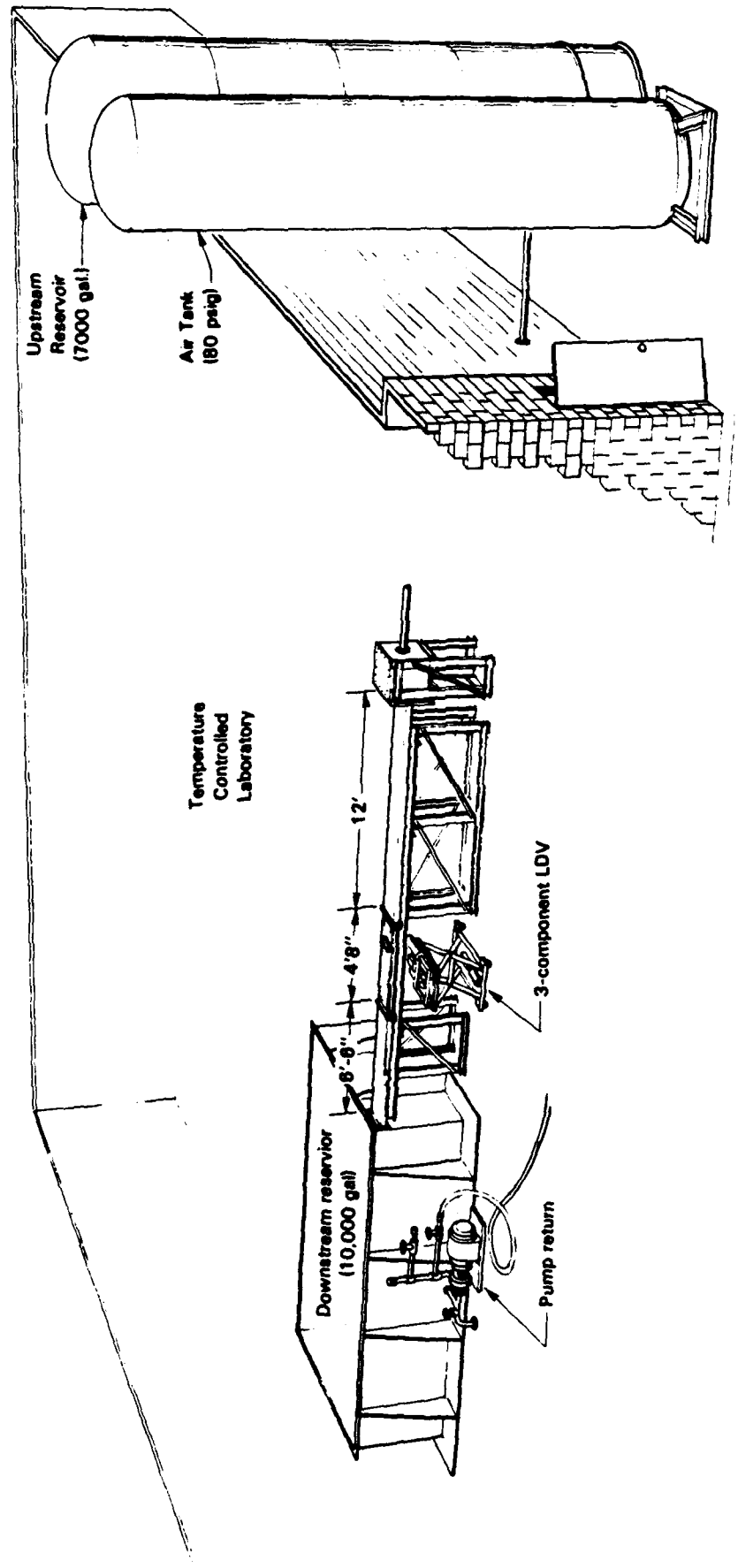


Figure 1. Rectangular Water Channel Facility.

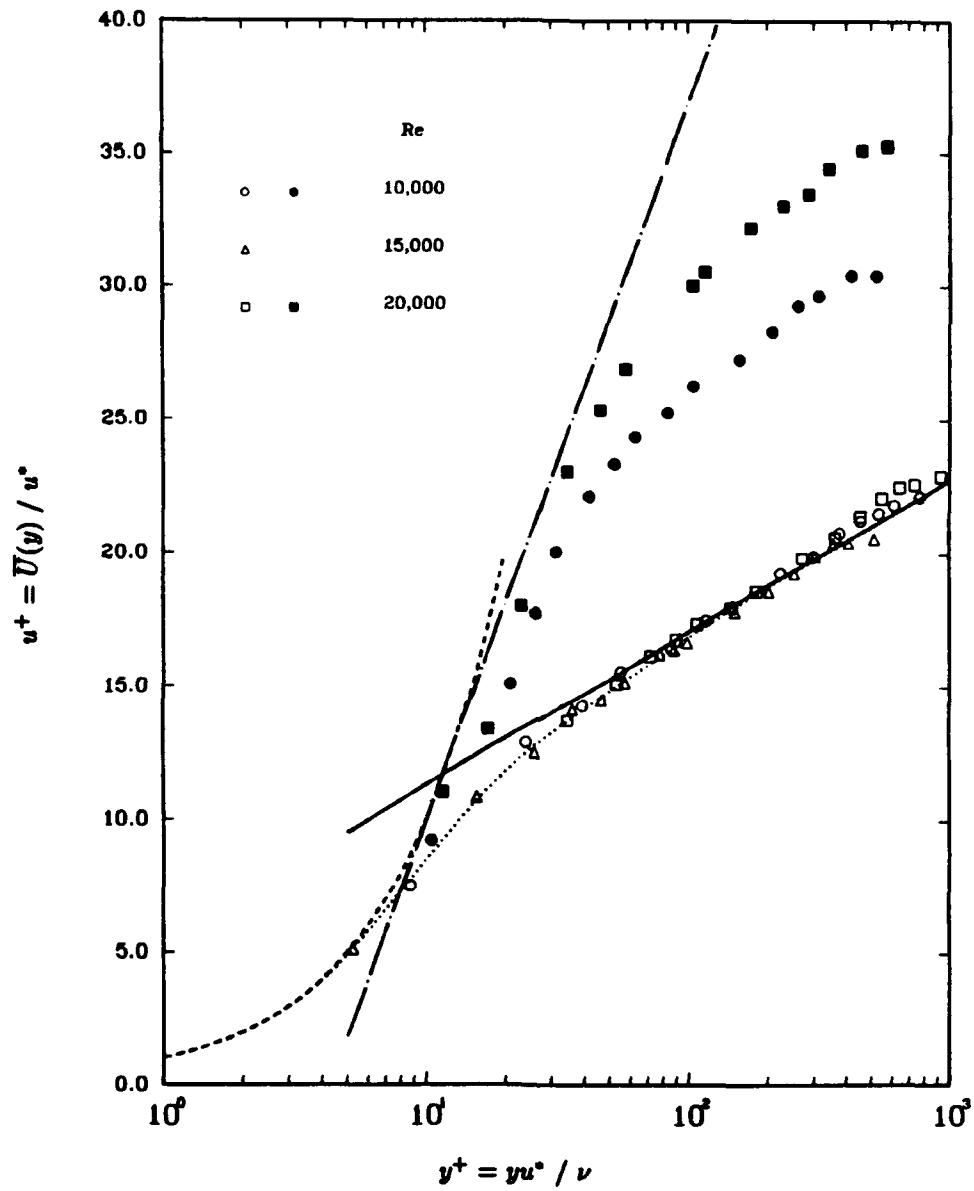


Figure 2. Mean Velocity Profiles For Newtonian (open symbols) and non-Newtonian (closed symbols): - - - - Law-of-the-wall; — Log-law; ····· Spalding¹⁵; —·— Virk¹⁷.

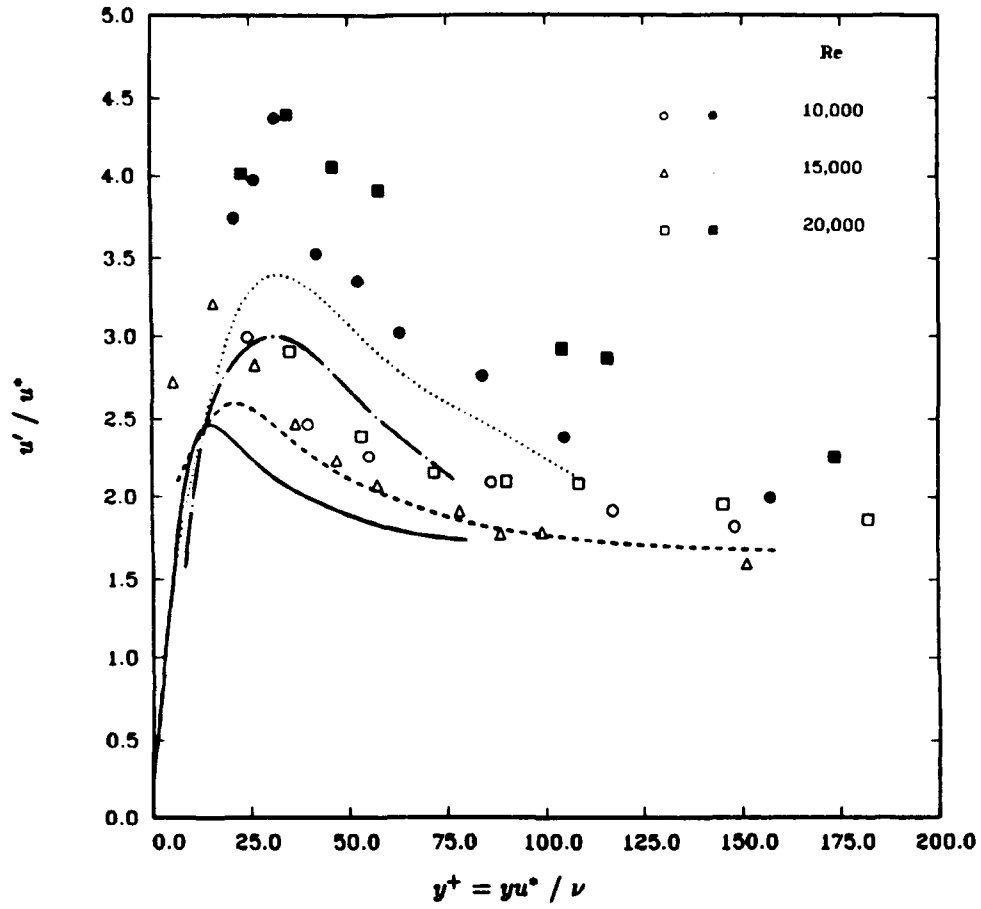


Figure 3. Turbulence Intensity Profiles For Newtonian (open symbols) and non-Newtonian (closed symbols): *Reischman&Tiederman*¹⁴
 ——— Newtonian and — · — non-Newtonian; *Wilmarth et al*²⁰
 - - - - - Newtonian and non-Newtonian.

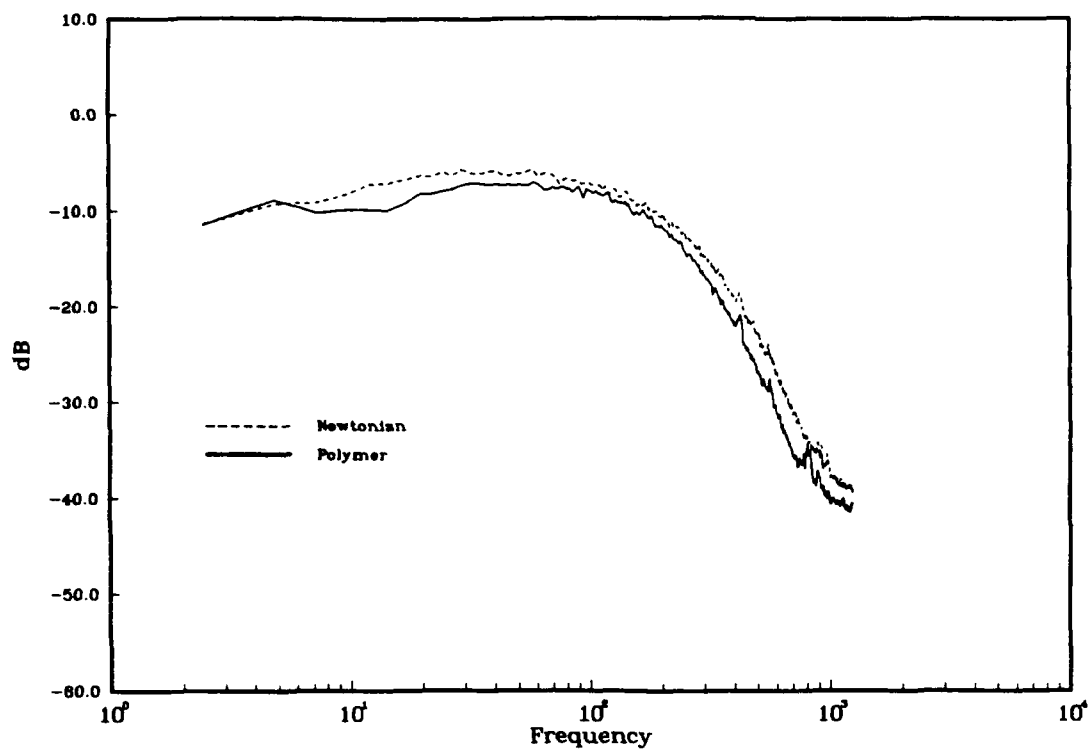


Figure 4A. Raw Spectral Output for $R_h = 15,000$ With 11.8% Drag Reduction.

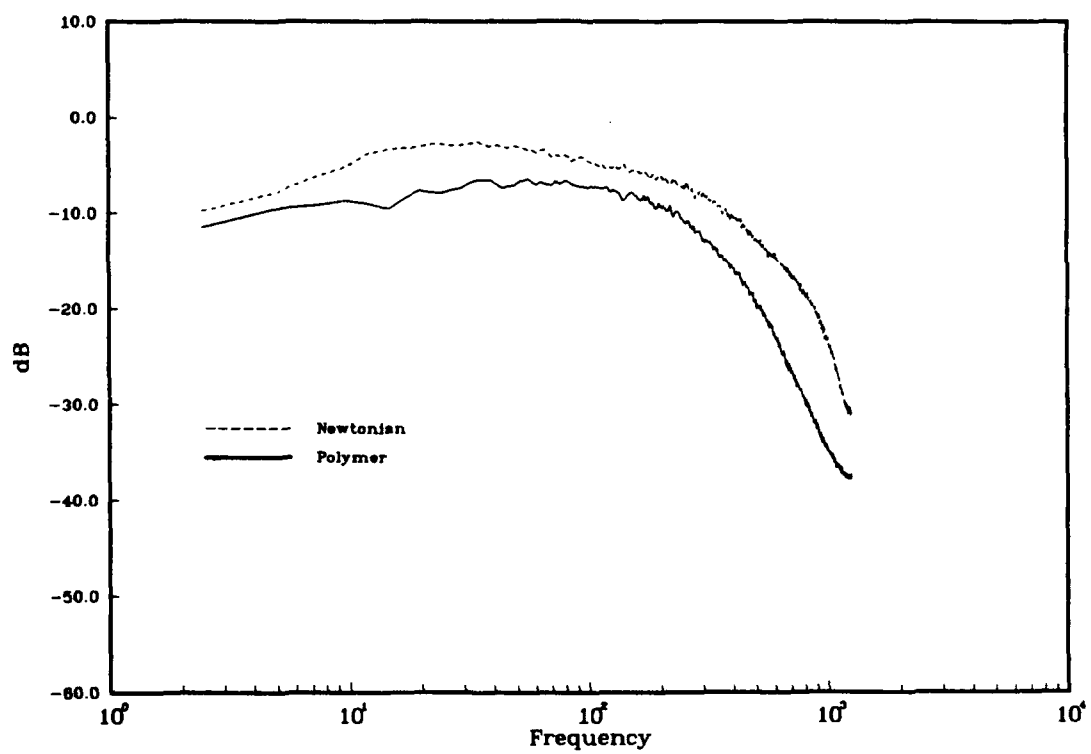


Figure 4B. Raw Spectral Output for $R_h = 20,000$ With 26.8% Drag Reduction.

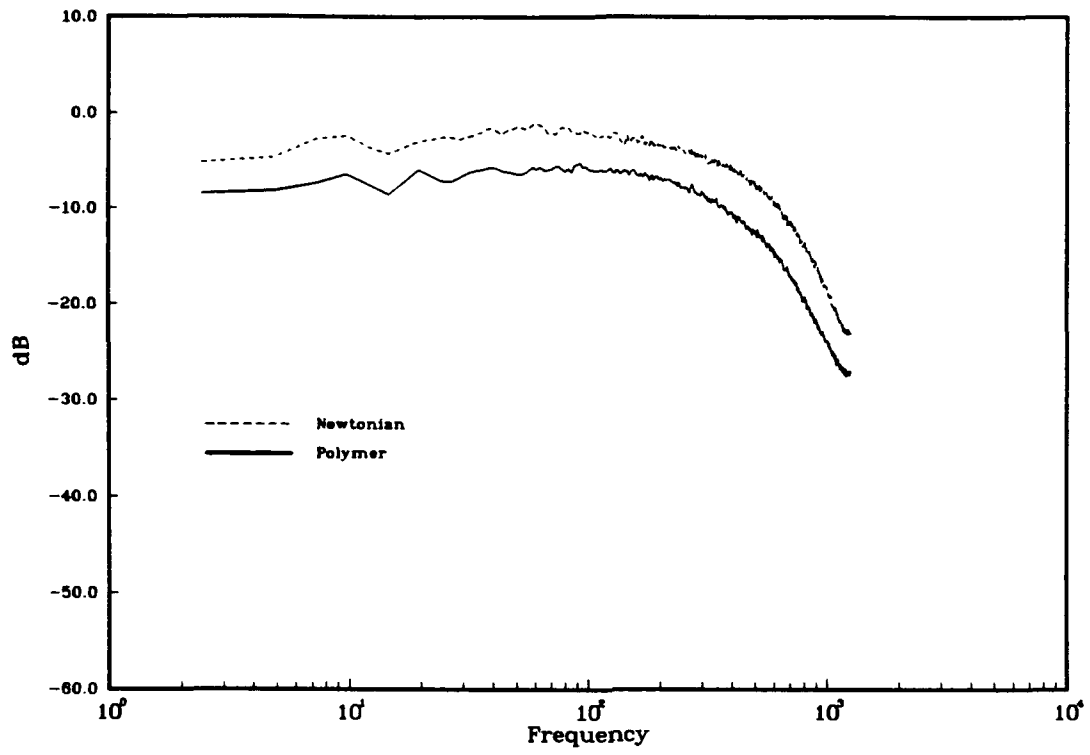


Figure 4C. Raw Spectral Output for $R_h = 25,000$ With 32.3% Drag Reduction.

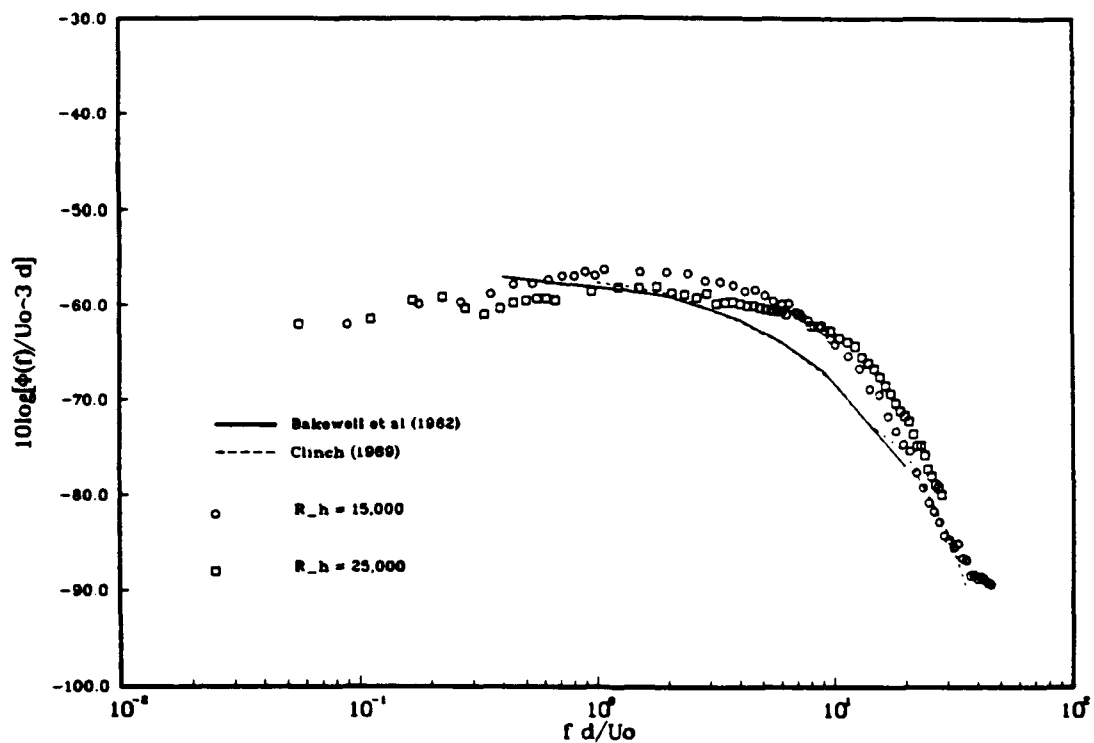


Figure 5A. Newtonian Composite Using Outer Variables.

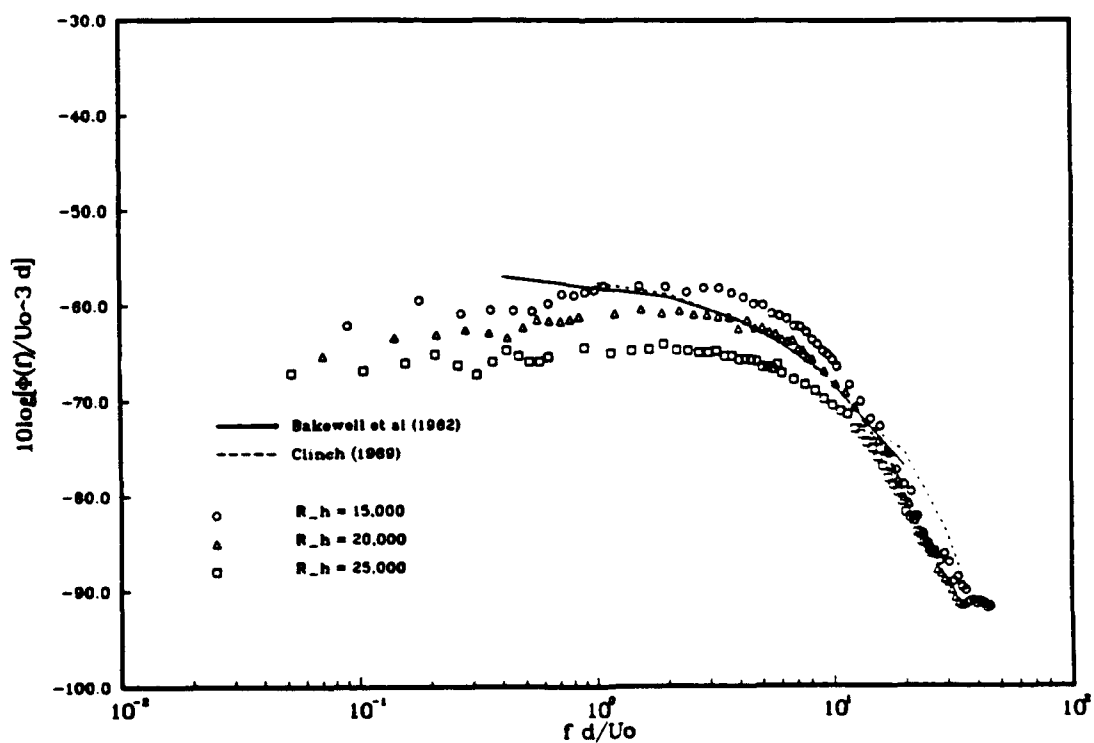


Figure 5B. Polymer Composite Using Outer Variables.

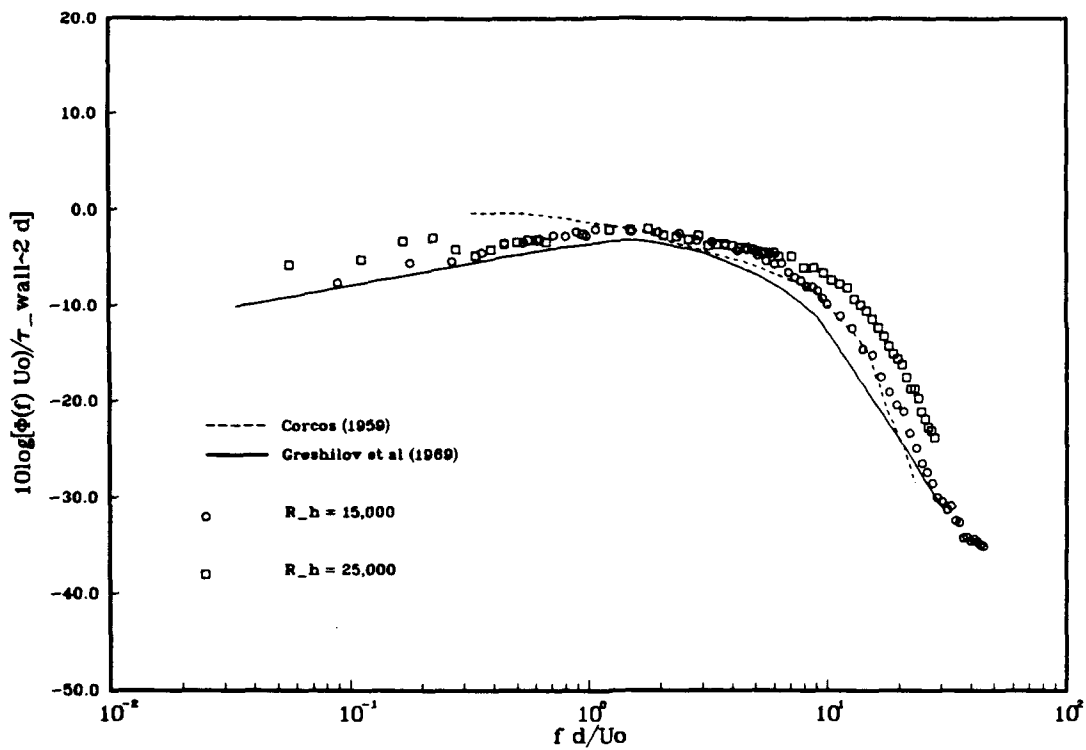


Figure 6A. Newtonian Composite using Mixed Variables.

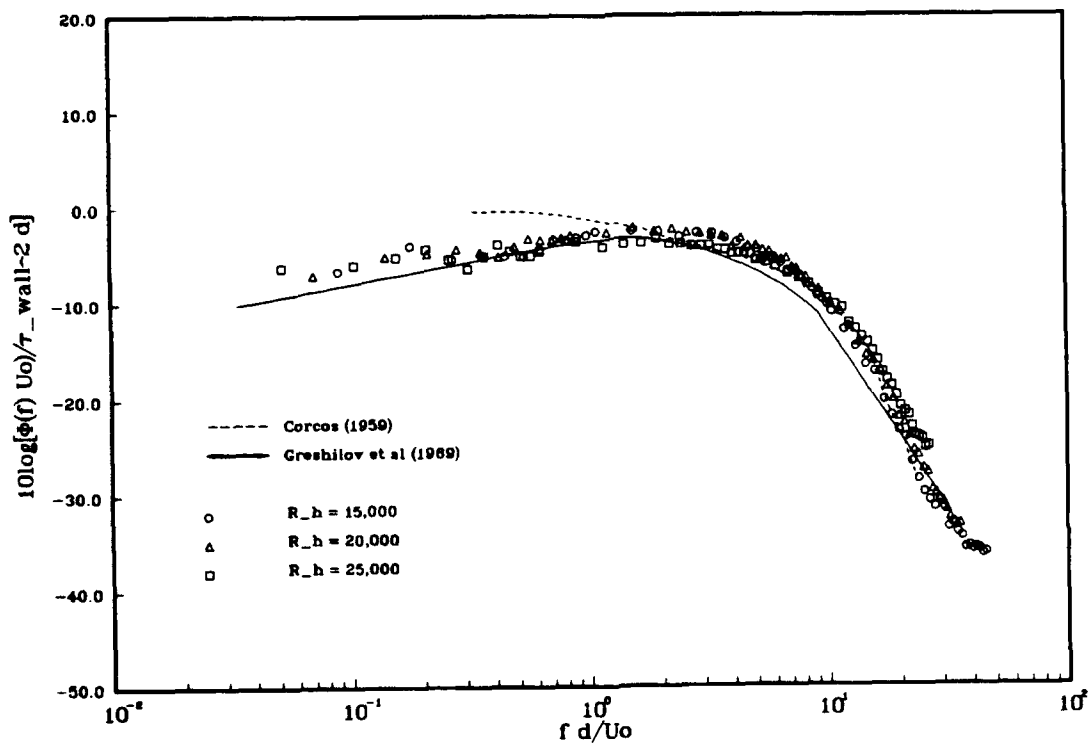


Figure 6B. Polymer Composite using Mixed Variables.

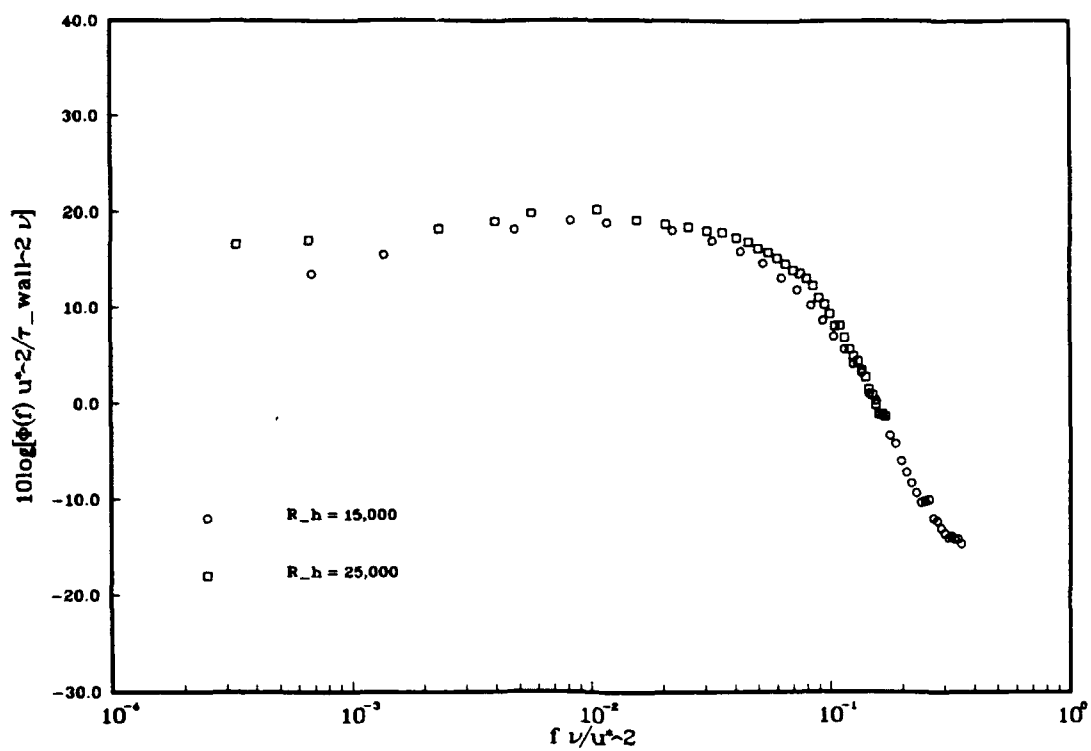


Figure 7A. Newtonian Composite Using Inner Variables.

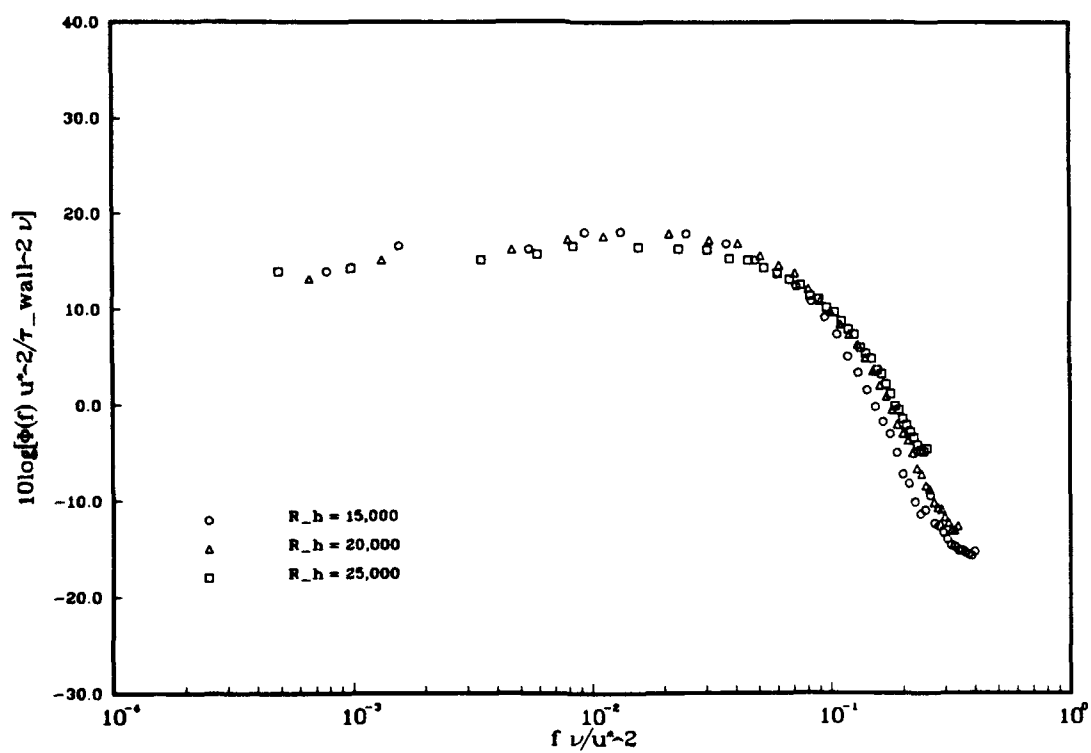


Figure 7B. Polymer Composite Using Inner Variables.

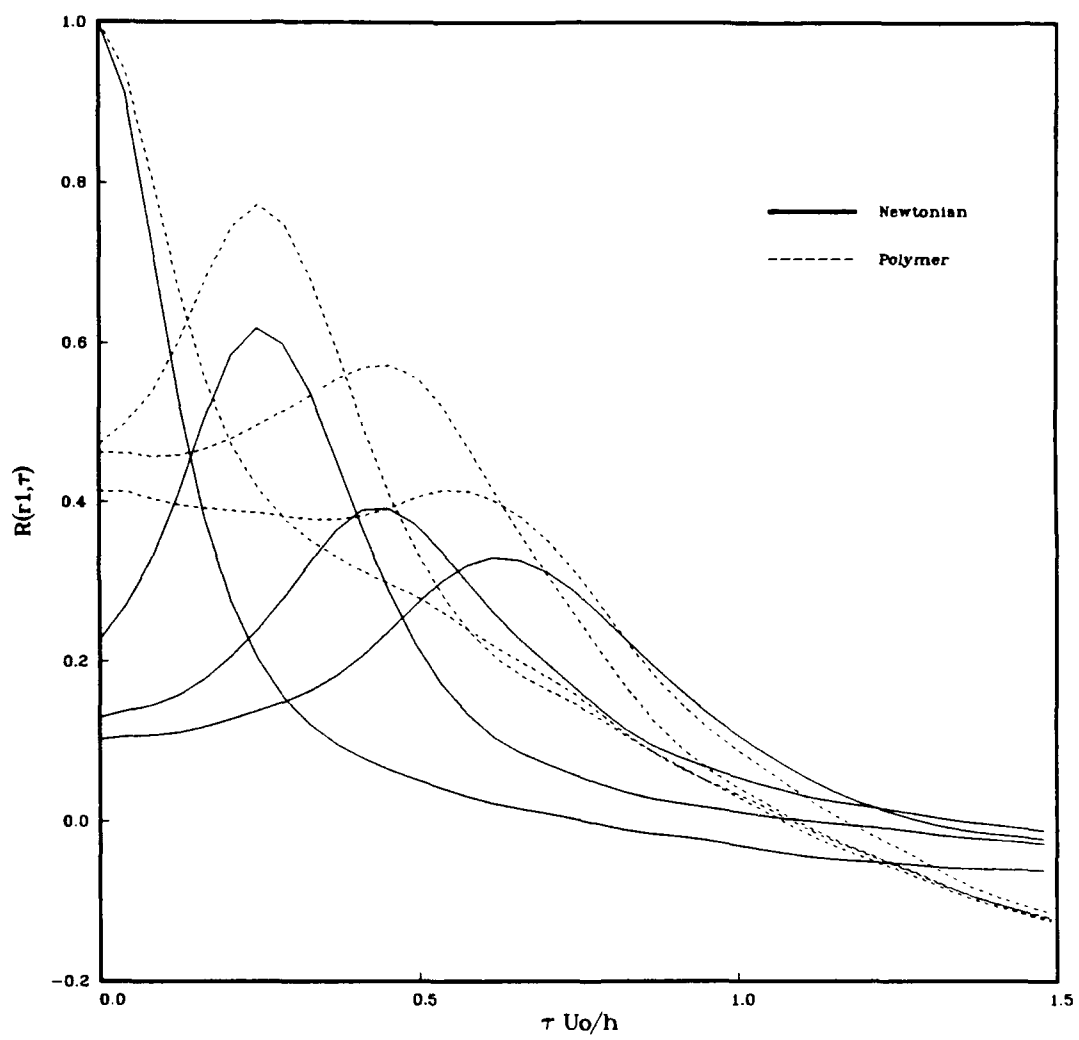


Figure 8A. Inline Correlation for $R_h = 15,000$.

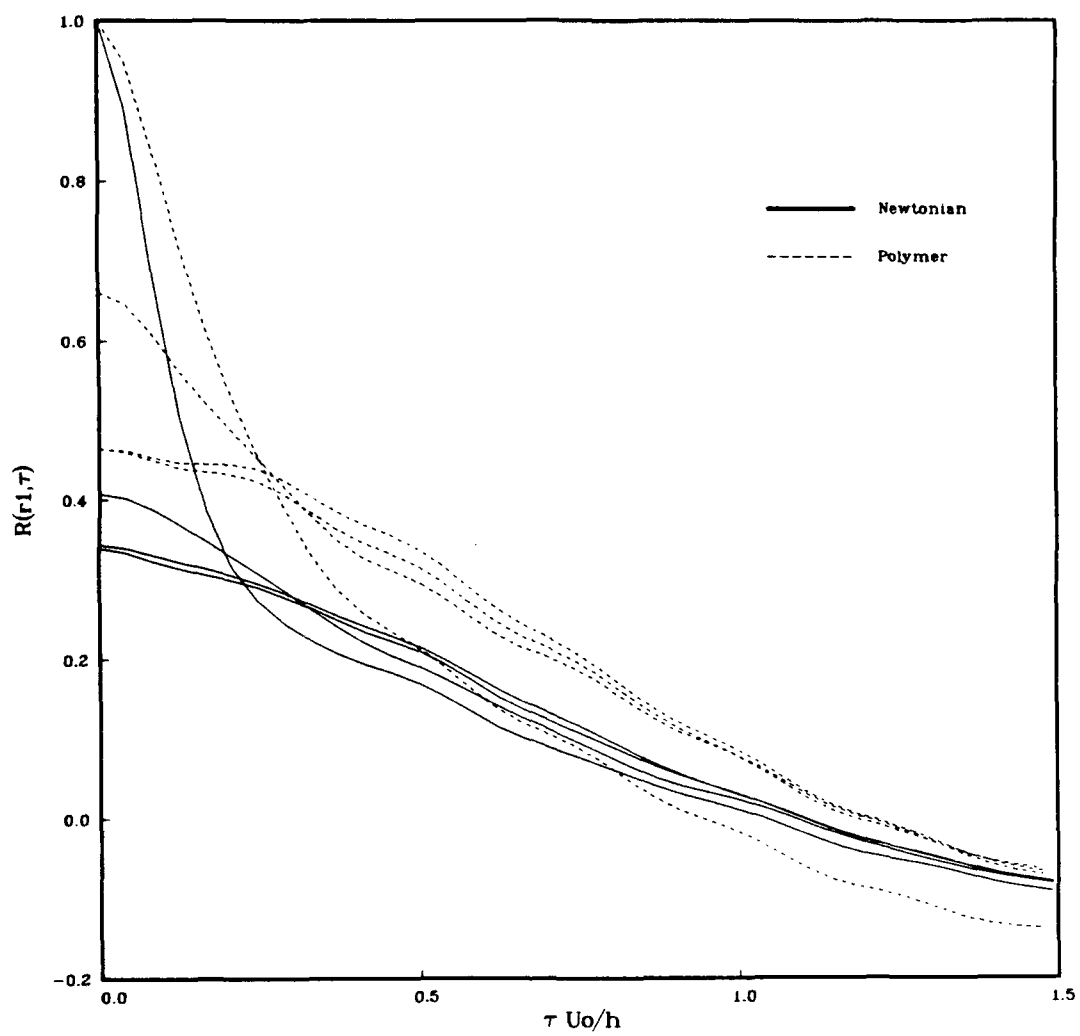


Figure 8B. Transverse Correlation for $R_h = 15,000$.

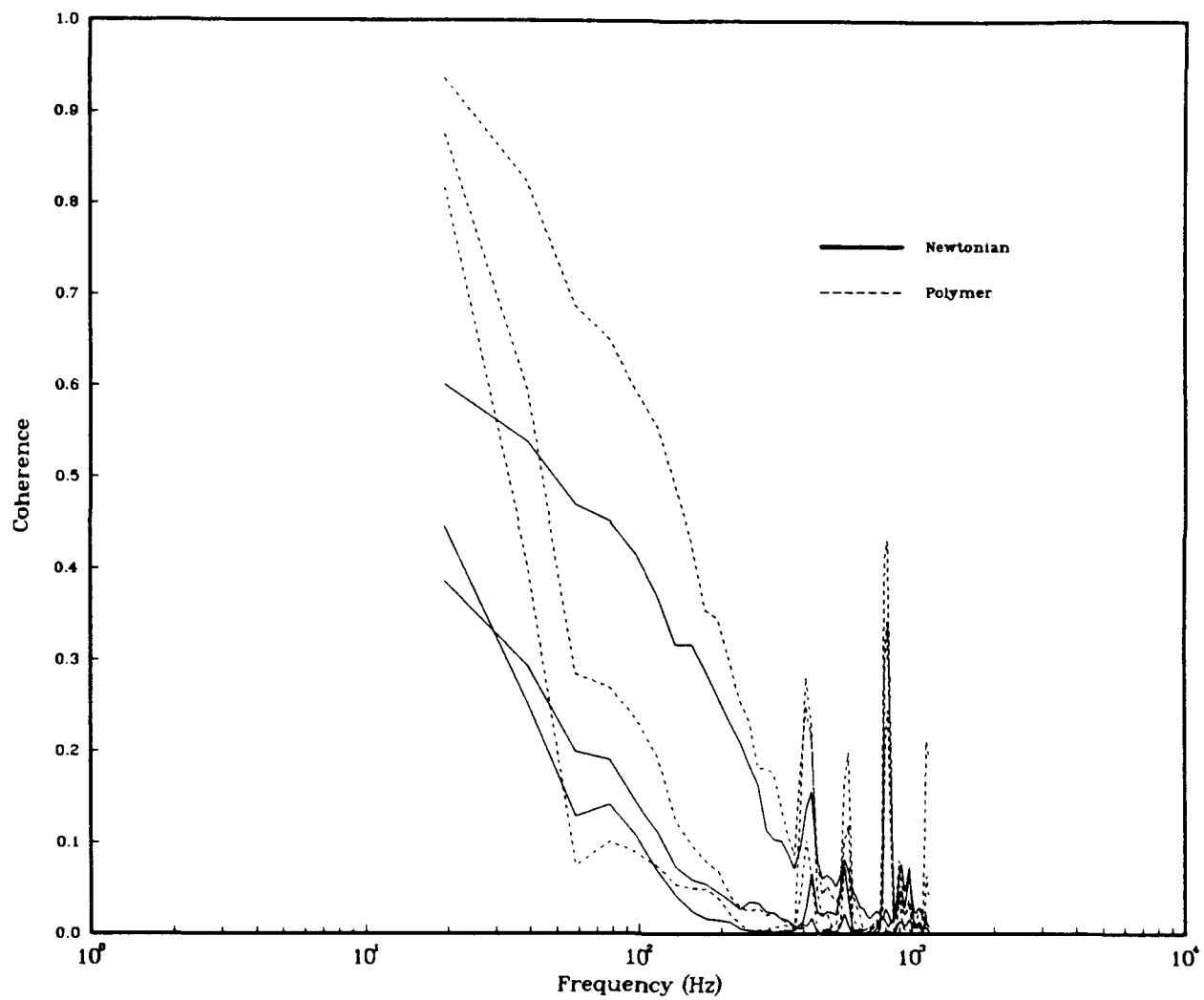


Figure 9. Inline Coherence for $R_h = 15,000$.